Schweizerische Eidgenossenschaft
Confédération suisse
Confederazione Svizzera
Confederaziun svizra

Federal Department of Home Affairs FDHA
Federal Office of Meteorology and Climatology MeteoSwiss

Weather forecasts, observations and algorithms for building simulation and predictive control

Contributions by MeteoSwiss for the 3rd year of OptiControl

Authors:
Vanessa Stauch, Christophe Hug, Francis Schubiger, Philippe Steiner

Federal Office of Meteorology and Climatology MeteoSwiss, Zurich, Switzerland

Version 3.0

Zurich, 30.07.2010

Vanessa Stauch
Krähbühlstrasse 58, 8044 Zurich
Phone +41 44 256 92 04, Fax +41 44 256 92 78
vanessa.stauch@meteoswiss.ch
www.meteoswiss.ch

Table of contents

1 Introduction

Predictive building automation applications pose a particular challenge for numerical weather prediction (NWP) models as they require accurate point forecasts for very local conditions at the building site. Therefore, efficient ways need to be developed that address and reduce the limitations of the NWP model by further (post-) process their output towards specifically tailored forecast products.

Given the growing knowledge of the project team about the studied building automation systems and their response to weather forecasts, the third year of OptiControl was devoted to further adapt and post-process the relevant weather predictions to the specific needs of the applications at hand. For this, statistical and physically based postprocessing schemes have been (further) developed for the operational NWP model COSMO-7 at MeteoSwiss (www.cosmo-model.org, Steppeler et al. 2003) that aim at providing the best possible point prediction for energy efficient building control.

In the following, we report on the various developments and studies carried out at MeteoSwiss during the final year of OptiControl. We start with a brief description of the implementation of the previously developed local correction (Cattani 1994, Stauch et al. 2010) into the operational forecasting system at MeteoSwiss (chapter 2). The correction is designed to affect the entire forecast range (three days for COSMO-7) and implicitly takes into account the daily cycle of temperature and radiation by using hourly observations of an entire day for each correction step. As the first few time steps (here one hour) of the weather forecasts proved to be most crucial for the control performance, chapter 3 introduces a short-term correction algorithm that uses the latest (hourly) observation only and explicitly models an autoregressive process for the forecast error. This algorithm has been implemented in the OptiControl simulation software BACLab to simulate the on-site correction where the local measurements are available. The effect of each correction and the combined scheme on the control performance in building automation is then investigated in chapter 4. The aim here is to better understand the sensitivity of the control system to uncertainties in the weather forecasts by studying the primary energy use and comfort violations in simulations for a range of buildings and sites. The subsequent chapter reports on yet another extension to BACLab for local and individual adaptation of the weather forecasts to the needs of the particular building application (chapter 5). It converts observations and predictions of (horizontal) global radiation into incident direct and diffuse radiation components on inclined surfaces (e.g. window façades) being required by the controller as disturbances. This way, the simulation of arbitrarily oriented buildings/rooms with a wide range of different window areas is possible which is particularly useful for the demonstrator building (orientation of 40° from north, see Sagerschnig et al. 2010). Also, specific site conditions such as the apparent horizon around a building can be taken into account, making the simulation software more flexible for new buildings. Finally, the last chapter describes the extensions of the OptiControl weather and occupancy database that includes the observations and COSMO-7 forecasts for the years 2008 and 2009 providing the basis for long-term building simulations with BACLab (chapter 4, Sagerschnig et al (2010) and possibly beyond the project OptiControl).

2 Statistical adaptation of COSMO predictions to local conditions: operational implementation

2.1 Motivation

Point predictions of NWP models can be systematically improved by the use of (past) local observations and suitable statistical models. In particular, recursive estimation of state space models with the Kalman filter (Kalman 1960) provide an appealing framework for online correction of forecast errors if actual observations are available (Cattani 1994). Given historic weather predictions and observations of the OptiControl weather and occupancy database (OCWDB), Stauch et al. (2010) demonstrate the feasibility of such models to adapt the COSMO-7 weather forecasts relevant for predictive building control to the specific local conditions. To provide improved forecasts for the controller at a specific

building in real-time (e.g. for the demonstrator), the correction scheme is being embedded into the operational COSMO forecast production scheme at MeteoSwiss where the latest COSMO forecast and actual local observations are readily available.

2.2 Overview of the operational scheme

The correction module has access to the MeteoSwiss observation database and the most recent COSMO forecasts. In turn, the Kalman filter core delivers all necessary information to the software (fieldextra) that carries out the correction of the current COSMO forecast. All updated matrices and vectors of the state-space model are stored in an internal database to be available for the next update step once new observations become available (*Figure 2.1*). A flexible design and the choice of an object oriented programming approach allow to easily extending the package for new stations, and also for new parameters provided an appropriate error model has been identified. This way, local adaptation of the radiation components will be included following Stauch et al. (2010) provided the simulation study in chapter 4 shows a benefit for predictive building automation applications.

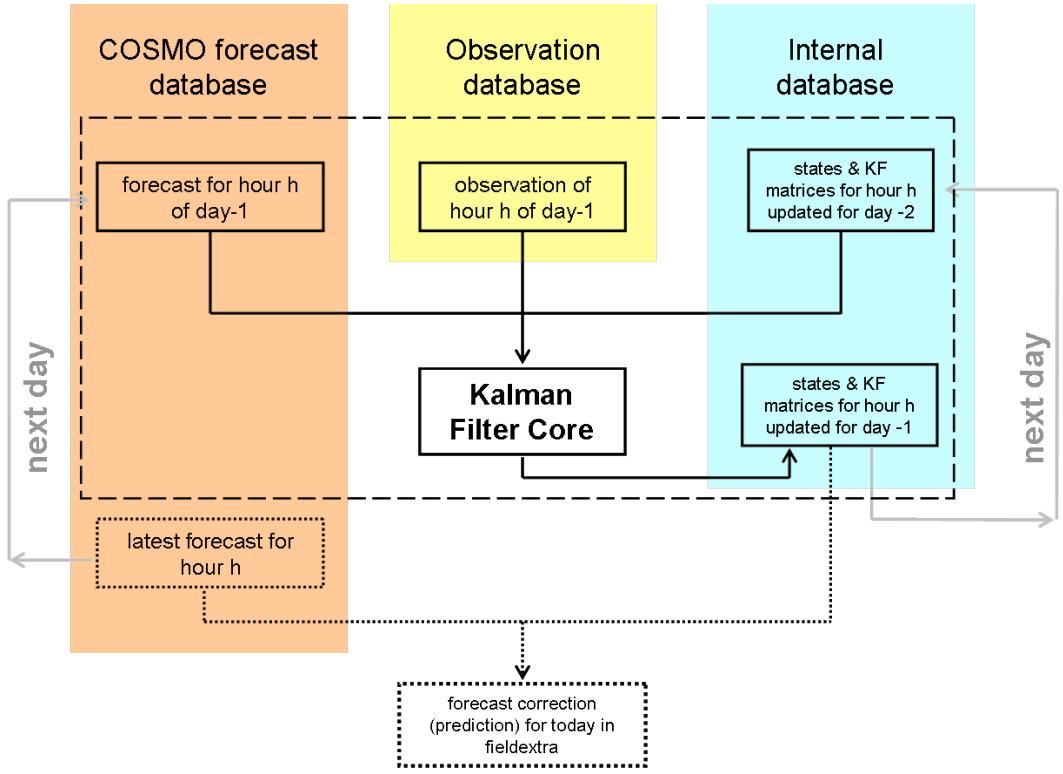

Figure 2.1: Schematic diagram of the operational correction module, the dashed line denotes the module itself, the dotted lines indicate the processes directly connected to the module via the software fieldextra and the grey arrows illustrate the next time step.

2.3 Conclusions

The developed adaptation module enables to correct the COSMO predictions operationally for any location where measurements are available online. By the end of the OptiControl project, the envisaged demonstrator building will benefit from the improvements as real-time adapted point predictions will be provided. With the ongoing expansion of the measurement network, such improved point predictions will become available for a more and more dense mesh of observation sites.

3 Short-term correction of weather predictions at building site

3.1 Motivation

The improved point forecasts of COSMO-7 can serve now as input for the controller where they are used as disturbance predictions. However, the update frequency of the controller for the optimisation of the next control action (here one hour) is smaller than the update frequency of the COSMO-7 forecast runs (here 12 hours). Between these COSMO-7 updates, new observations at the building become available that could help to characterise the model's actual prediction error and ultimately to further correct the subsequent (few) forecast hours. As the controller's performance has been shown to be particularly sensitive to the accuracy of the first hours of the predictions, the aim of this chapter is to develop a statistical model that improves the COSMO-7 predictions with the use of the latest observations at the building site.

3.2 The correction algorithm

The COSMO-7 forecast error particularly for radiation variables is characterised by a high variability that can be related to model error but also to temporally and spatially fast changing cloud formation and dissolving processes being effective on smaller scales than the COSMO-7 resolution. However, these processes are naturally correlated and we exploit this property by formulating an autoregressive model to describe the errors of point forecast. Given the forecast error is changing with the changing weather situation, also the degree of autocorrelation can be expected to vary in time. Denoting y_h as the forecast error at time *h*, the above described error properties can be formulated as the following state-space model,

$$x_h = x_{h-1} + w \qquad \text{with } w \sim N(0, Q) \tag{3-1}$$

$$y_h = x_h y_{h-1} + v \qquad \text{with } v \sim N(0, R) \tag{3-2}$$

with x_h being the time varying autocorrelation coefficient at time *h* following a random walk. This simple model has been chosen as no other information is available. w and v are serially uncorrelated white noise processes with time invariant variances Q and R, respectively. Their values are chosen based on old data. The performance of the correction appears to be only sensible to the magnitude of the signal to noise ratio (Q/R) which could be automatically optimised in future implementations. The temporal evolution of the autocorrelation coefficient x_h is estimated recursively with a linear discrete Kalman filter. Additional upper and lower limits for the value of x_h are introduced in order to ensure a nonstationary process. An example of the dynamic behaviour of x_h for the three disturbance variables for the controller is shown in Figure 3.1.

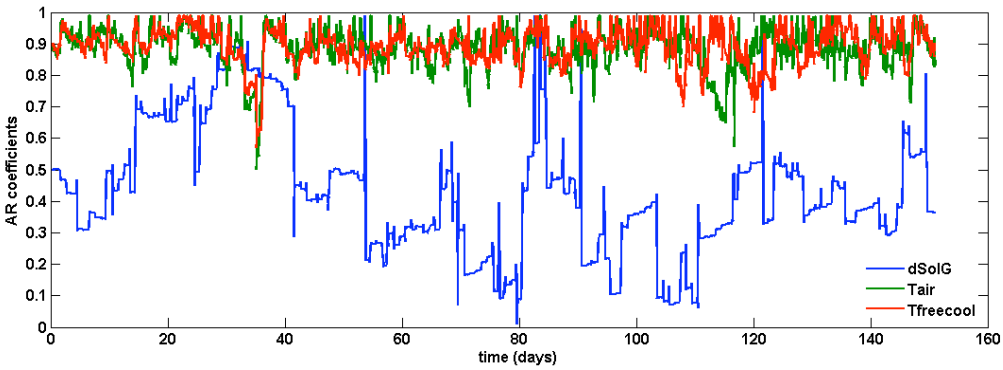

Figure 3.1: Temporal evolution of the hourly autocorrelation coefficient for the three meteorological input variables to the controller for 150 days in 2007 for Zurich. While the two temperature variables (Tair, Tfreecool) show somewhat stable autoregressive behaviour, the coefficient for the solar heat gain (dSolG) significantly varies over time.

Model (3-1 and 3-2) has proved beneficial for all required input weather variables and can be applied on all disturbance variables for the controller. It has been implemented in the BACLab software to mimic the control of a real building where on-site measurements (as opposed to observations at a meteorological station being available at MeteoSwiss) would be used to adapt the weather forecasts to the local conditions.

3.3 Evaluation of the performance

The performance of this correction algorithm is evaluated by means of the systematic error (bias) and the standard deviation of the COSMO-7 forecast error as a measure of accuracy. To assess the effect of the correction as a function of lead time and as a function of the time of day, a forecast matrix is used that contains hourly COSMO-7 forecasts up to a prediction horizon of maximal 60 hours with an artificial hourly update. As a result, for the hours between two COSMO-7 updates at 00 and 12 UTC, "old" forecasts are recycled to provide hourly updates for the controller (Figure 3.2).

Hour	**COSMO-7 run**	**+00**	**+01**	**+02**	**+03**	**+04**	**+05**	**+06**	**+07**	**+08**	**…**
01	00 UTC	+01	+02	**+03**	+04	+05	**+06**	+07	+08	+09	…
02		+02	**+03**	+04	+05	**+06**	+07	+08	+09	+10	…
…	…										…
11		+11	+12	+13	+14	+15	+16	+17	+18	+19	…
12		+12	+13	+14	+15	+16	+17	+18	+19	+20	…
13	12 UTC	+01	+02	**+03**	+04	+05	**+06**	+07	+08	+09	…
14		+02	**+03**	+04	+05	**+06**	+07	+08	+09	+10	…
…	…										…
24		+12	+13	+14	+15	+16	+17	+18	+19	+20	…

Figure 3.2: Design of a forecast matrix for one day within BACLab. The rows denote the current time (UTC), the columns are the lead times for the controller. The matrix entries indicate the lead time of the respect COSMO-7 prediction. Green text colour underlines the shift of the predictions.

As expected, the impact of the correction is largest for the first few hours of the predictions as highlighted in Figure 3.3 for an averaged 10 days time series for solar heat gain predictions. The predictions for longer lead times are left unchanged as the current measured value provides no information about the expected errors for the say following days.

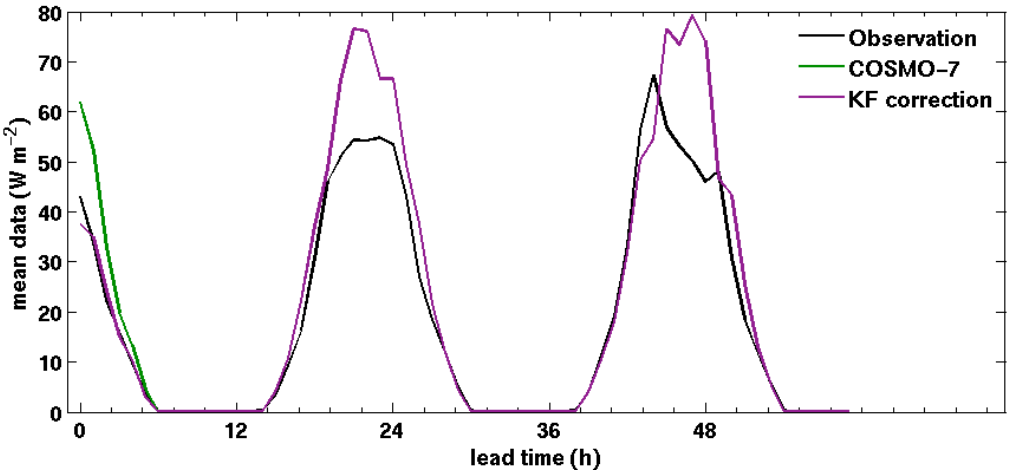

Figure 3.3: Example of the impact of the local correction on the COSMO-7 predictions for the solar heat gain on south orientated windows at Zurich, 01.07.-10.07.2007. Systematic improvements are dominant in the first few hours of the forecast. The green COSMO-7 predictions are covered by the predictions after the correction has been applied for the subsequent hours as the correction loses its impact.

In-depth analyses of longer datasets disclose a dependency of the COSMO-7 forecast performance on the hourly start time of the forecast for the controller and the lead time (upper two panels in Figure 3.4). Note, that in this illustration, the daily cycle along the y-axis is shifted downwards when moving towards longer lead times. For example, the forecast for the start time 5UTC and the lead time 5h is valid for 10UTC. This explains the somewhat diagonal shape of the values of the verification scores. Obviously for the night tie, the error is zero. The systematic error of the predictions is also close to zero for the late afternoon before sun set and the morning after sun rise. The largest differences between the COSMO-7 predictions and the observations are found during mid-day. The comparison of the values for the systematic errors and the standard deviation of the error again underpins the comparatively large uncertainty in the radiation predictions. Interestingly, this verification uncovers a rather dominant difference between the two initial times for the COSMO-7 runs used here. Both, the systematic error and the standard deviation appear to be larger for the COSMO runs initialized at 12UTC than for the 00UTC runs. This is an interesting result and will be further investigated at MeteoSwiss.

The lower panels in Figure 3.4 show the benefit of the local correction in terms of the difference between the absolute bias and standard deviation of the DMO and the corrected forecasts. When averaged over the entire year, the effect of the correction on the forecast quality holds for up to four forecast hours. The positive effect on the variability of the forecast error fades out a little earlier. Close examination of the difference in the bias uncovers that the success of the correction for the hours from 10 to 12 appears to be larger than for the hours from 12 to 16. A reason for this might probably lie in the set-up of the correction algorithm that does not explicitly take into account the “discontinuity” of COSMO-7 forecasts from 11 to 12UTC. However, the improvements are significant and it will be interesting to investigate how these changes propagate through the predictive building control system and its performance (chapter 4.2).

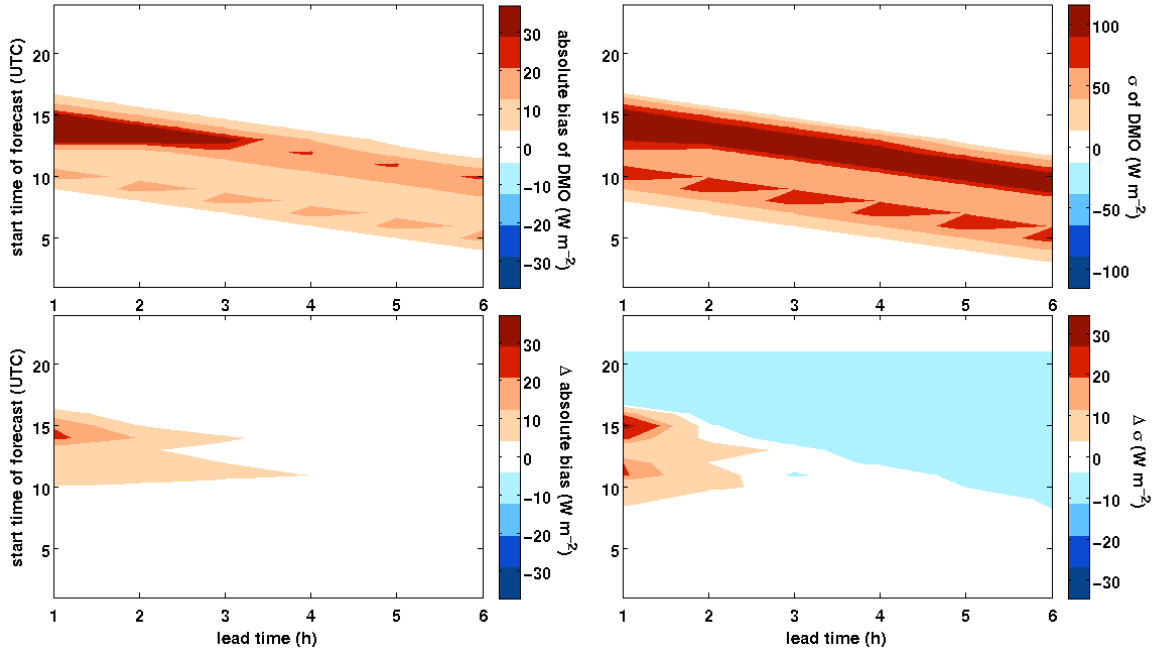

Figure 3.4: Mean effect of the correction for solar heat gain predictions for the entire year 2007 at Zurich. Simulated is the input for a standard Swiss average building with south orientation and a wide window area fraction. The upper two panels show the absolute bias (on the left) and the standard deviation, σ (right) for the uncorrected COSMO-7 predictions (DMO) over the day (start time of the forecast, y-axis) and as a function of (short) lead time (x-axis). The lower panels show the difference between the DMO and the corrected COSMO-7 predictions for the same two scores. Red colors in the bottom panels indicate an improvement of the scores.

3.4 Conclusions

Simulation results have shown the high importance of the forecast quality in the first few hours of the prediction horizon for the building automation systems under study. Therefore, the use of the most recent observation in combination with a suitable statistical model to correct the latest forecast is expected to significantly improve the control performance (Oldewurtel et al. 2010). A more comprehensive simulation study to investigate this impact is outlined in chapter 4. The extension of the BACLab software by this short-term correction gives the opportunity to simulate the realistic scenario of a real-time correction at the building site where the local observations are readily available.

4 Sensitivity of predictive building automation to weather forecasts

4.1 Motivation

The expected energy savings potential of predictive control have shown to be highly variable when simulating integrated room automation for a range of buildings and climates (Gwerder et al. (2010), Gyalistras et al. (2010)). These studies have in common the use of perfect weather predictions in order to quantify the benchmark for the predictive controllers. Stauch et al. (2008) and Oldewurtel et al. (2010) have presented first results of 'real world' simulations, i.e. (model-) predictive control simulations using operational weather forecasts of COSMO-7, and show for a small number of simulation cases to what extend the potential energy savings potential can be exploited given uncertain predictions. Here, these results will be extended to a more comprehensive simulation study that aims to investigate the sensitivity of predictive control performance to the uncertainty in the weather predictions. In particular, the effect of the different correction steps of the forecasts on the primary energy usage and comfort violations and the relative importance of the 3 weather variables (air temperature, wetbulb temperature and global radiation) will be investigated for a range of buildings and sites.

The following abstract has been submitted for presentation at the European Conference on Applied Climatology 2010. The results and their discussion will complete this chapter in the final version of this report.

4.2 Tailored high-resolution numerical weather forecasts for energy efficient predictive building control

The high proportion of the total primary energy consumption by buildings has increased the public interest in the optimisation of buildings' operation and is also driving the development of novel control approaches for the indoor climate. In this context, the use of weather forecasts presents an interesting and – thanks to advances in information and predictive control technologies and the continuous improvement of numerical weather prediction (NWP) models – an increasingly attractive option for improved building control.

Within the research project OptiControl (www.opticontrol.ethz.ch) predictive control strategies for a wide range of buildings, heating, ventilation and air conditioning (HVAC) systems, and representative locations in Europe are being investigated with the aid of newly developed modelling and simulation tools. Grid point predictions for radiation, temperature and humidity of the high-resolution limited area NWP model COSMO-7 (see www.cosmo-model.org) and local measurements are used as disturbances and inputs into the building system. The control task considered consists in minimizing energy consumption whilst maintaining occupant comfort.

In this presentation, we use the simulation-based OptiControl methodology to investigate the impact of COSMO-7 forecasts on the performance of predictive building control and the resulting energy savings. For this, we have selected building cases that were shown to benefit from a prediction horizon of

up to 3 days and therefore, are particularly suitable for the use of numerical weather forecasts. We show that the controller performance is sensitive to the quality of the weather predictions, most importantly of the incident radiation on differently oriented façades. However, radiation is characterised by a high temporal and spatial variability in part caused by small scale and fast changing cloud formation and dissolution processes being only partially represented in the COSMO-7 grid point predictions. On the other hand, buildings are affected by particularly local weather conditions at the building site. To overcome this discrepancy, we make use of local measurements to statistically adapt the COSMO-7 model output to the meteorological conditions at the building. For this, we have developed a general correction algorithm that exploits systematic properties of the COSMO-7 prediction error and explicitly estimates the degree of temporal autocorrelation using online recursive estimation. The resulting corrected predictions are improved especially for the first few hours being the most crucial for the predictive controller and, ultimately for the reduction of primary energy consumption when using predictive control.

The use of numerical weather forecasts in predictive building automation is one example in a wide field of weather dependent advanced energy saving technologies. Our work particularly highlights the need for the development of specifically tailored weather forecast products by (statistical) postprocessing in order to meet the requirements of specific applications.

5 Direct and diffuse radiation on inclined and oriented surfaces

5.1 Motivation and introduction

The solar radiation has a significant impact on two aspects of the control task, the room temperature (solar heat gain) and users comfort (illuminance). While the direct radiation component contributes significantly to the heat budget within the room at no costs, the user might be disturbed by the beam if the current sun angle is adverse and there is no additional glare protection installed. As has been shown by Gwerder et al (2010), blind operation restrictions have a high impact on the control performance and therefore, the blind control plays an important role in energy efficient building automation. In order to optimize blind usage for heating and cooling purposes while maintaining glare protection with the same device, direct and diffuse solar radiation need to be distinguished for blind control. As a result, accurate knowledge of the global radiation and its components incident through the window area is a prerequisite for such advanced control strategies.

Starting from global radiation values, two steps are necessary for the derivation of radiation components on inclined and oriented surfaces. First, the global radiation has to be disaggregated into a direct and a diffuse component. Many algorithms of various complexity and nature have been proposed in the literature (e.g. Erbs et al. (1982), Skartveit & Olseth (1987), Perez et al. (1992)). A recent comparison and evaluation of the models with measurements suggests the Perez model to be outperforming the others included in the study (Ineichen 2008). This model has been chosen for the reference datasets in guidelines and standards of the Swiss Association of Engineers and Architects (SIA Merkblatt 2028, 2008) that has been particularly designed for building physics, energy and building technology and is also being used in OptiControl (Stauch et al. 2010). Second, the diffuse (and direct) component needs to be adapted to tilted surfaces (e.g. windows) taking into account only the sky fraction for the diffuse radiation that is “visible” for the particular surface at a given point in time. Perez et al. (1987) proposed such a model that has been chosen for the simulations within OptiControl. While so far, this disaggregation and conversion has been performed outside the simulation software BACLab and stored in the OptiControl database for only four specified façades (vertical south, west, north, east), the current developments and implementation in BACLab enables a flexible use of this algorithm for any location and building as the specific local conditions (geographical coordinates, apparent horizon, orientation and inclination of the window area) can be individually taken into account. Within OptiControl, the resulting variables will be used to explicitly simulate (predictive) glare protection in the demonstrator building (Sagerschnig et al. 2010).

5.2 Disaggregation of global radiation into direct and diffuse radiation

The implemented disaggregation scheme makes use of a stability index to account for the dynamics of the atmospheric state (Perez et al. 1992). This requires besides a multidimensional empirical look-up table the values of the global radiation and the dewpoint temperature for the previous time step and, if available, for the subsequent time step to characterize the expected evolution of the atmosphere. Obviously, if measurements are being converted in real-time, future radiation and dewpoint temperature values are not available and the algorithm reduces to the consideration of the past time step only. On the contrary, radiation and dewpoint temperature predictions provide an estimate of the future radiation and the full algorithm can be exploited. The impact on the global radiation is small for most of the time but can be significant particularly for instable atmospheric conditions (Figure 5.1).

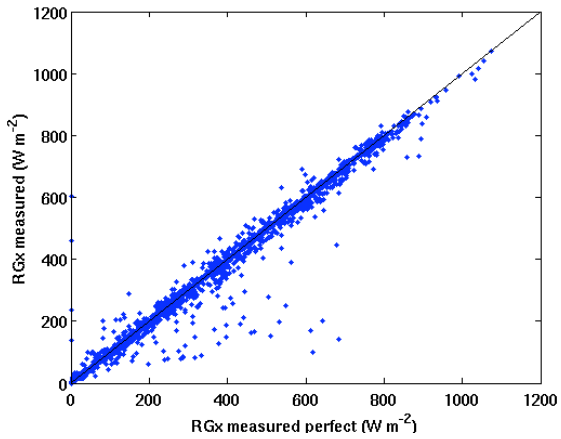

Figure 5.1: Differences between derived global radiation with the knowledge of the future value (e.g. when converting predictions) and without the knowledge of the future value (e.g. when converting actual measurements) for hourly values of the measured radiation at Basel in 2006. Here, RGx denotes the global radiation for vertical orientation south.

This disaggregation algorithm has been initially developed to convert global radiation measurements into direct radiation for solar energy and building climate applications. Numerical weather prediction models like COSMO comprise complex radiation sub-models that typically represent the most important physical processes involved in three-dimensions for the simulation and prediction of the temporal dynamics (Steppler et al. 2003). Obviously, the direct and diffuse radiation is explicitly modeled within COSMO and could be readily used as input for the calculation of radiation components on tilted surfaces. For OptiControl, these predictions have not been available as they were not archived between 2006 and 2008 and the global radiation predictions had to be converted following Perez et al. (1992). Since spring 2009, an extension of the radiation model has been implemented in COSMO that explicitly accounts for the effects of the complex topography of the Alpine domain (shadowing effects of the mountains) leading to better predictions of the radiation budget and its components (Buzzi 2009). Future applications (e.g. the operation of a demonstrator building) will benefit from this improvement that provides more consistent COSMO predictions for the diffuse and direct radiation.

5.3 Global, diffuse and direct radiation for inclined and oriented surfaces

Once the direct and diffuse component of the incident radiation is available, the specific characteristics of the building under study need to be taken into account for the derivation of the radiation input relevant for the building climate (Perez et al. 1987). The new radiation package within BACLab uses besides the geographical coordinates of the building site for the calculation of solar geometry, measurements of the apparent horizon around the building for the conversion of the diffuse and direct radiation on a surface of a given orientation and inclination. Again, optimized but empirical coefficients are used to describe the brightness and clearness of the overarching sky that can be found in Perez et al.

(1987). The package is used for both, observations and COSMO predictions and returns the global radiation as well as the diffuse and direct radiation component on an individually oriented and inclined surface.

5.4 Verification of the new radiation components

The main difference between the algorithm implemented in the BACLab Software and used for the datasets included in the OCWDB is the possibility to use more detailed information of the horizon surrounding the building following Buzzi (2009). Also, the improved “longterm” correction algorithm described in Stauch et al. (2010) and referred to in chapter 2 has been used to adapt the dewpoint temperature predictions as input to the algorithm. Finally, BACLab interpolates the instantaneous dewpoint temperature and albedo values into hourly averages (for hourly data sets). Because of these differences, we recommend to use the BACLab algorithm in any future simulation study in order to ensure consistency.

The differences between the observed and forecast global radiation will be propagated through the radiation conversion algorithm and will reappear in the derived radiation components. As the radiation conversion is highly nonlinear, a separate verification exercise is shown in *Figure* 5.2. Interestingly, the systematic overestimation during the morning and the afternoon and the slight systematic underestimation around midday by the global radiation COSMO-7 forecasts are not maintained through the conversion. Rather, the direct component is systematically underestimated in the afternoon and the diffuse component is overestimated particularly around midday. The highest proportion of variability is attributed to the direct component although the differences in the absolute values of the direct and diffuse component are less pronounced. Possibly, the forecast of the direct radiation is more affected by the high variability in the cloud cover implicitly derived within the algorithm.

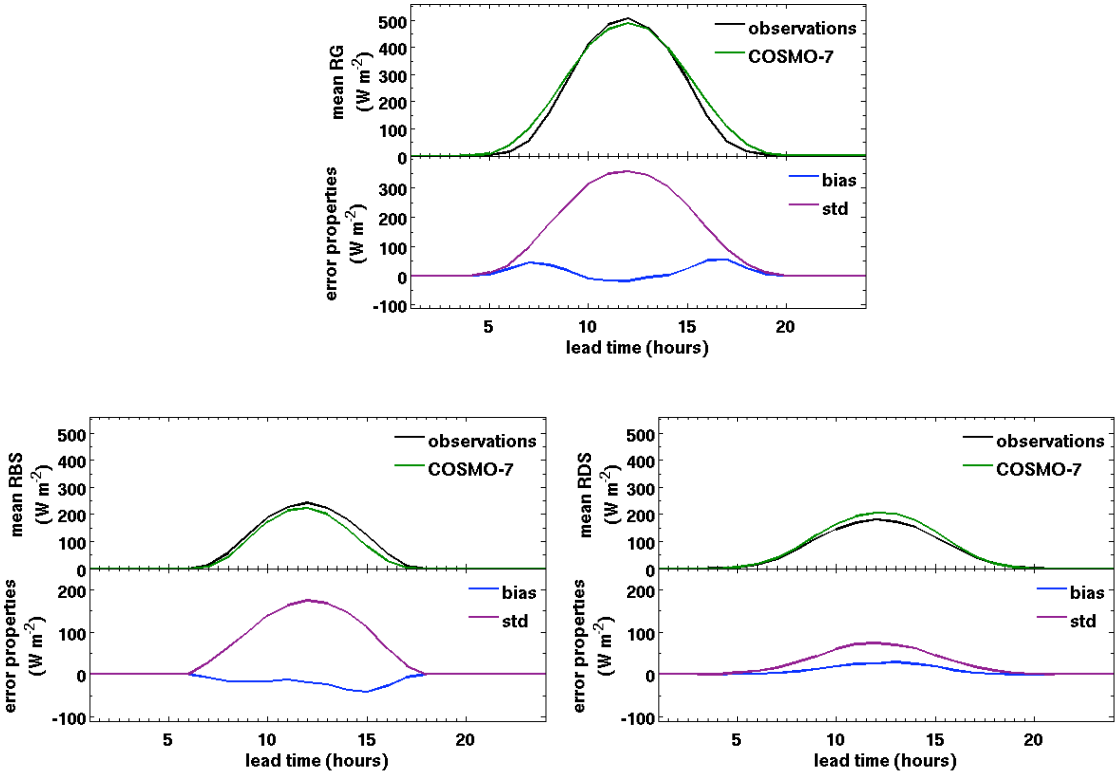

Figure 5.2*: Typical statistical properties of the global radiation forecast error compared to the properties after the conversion into direct and diffuse radiation on the façade averaged over all sites and the year 2009 and the COSMO-7 forecasts issued at midnight. The upper panel shows the average observed and forecast global radiation as well as the mean and the standard deviation as a function of lead time. The bottom panels show the same for the direct radiation component (left) and the diffuse component (right). Example for the orientation south.*

5.5 Conclusions

So far, only global radiation components on oriented surfaces were available, and only for the main directions (south, west, north, east) of vertical façades. The derived measurements and predictions were stored on the OCWDB that therefore limited the BACLab simulations to the respect buildings/rooms. The new radiation package extends the application range of BACLab to arbitrarily oriented and inclined surfaces and allows the use of horizon measurements at any building site (e.g. demonstrator building). Furthermore, the internal derivation of the direct and diffuse radiation on the window area enables the extension to the simulation and automation of glare protection being particularly interesting for office building applications.

6 Extensions of the OptiControl Weather and Occupancy Database

6.1 Motivation

As being typical for NWP models, the COSMO model undergoes a constant development and improvement. Since 2007, most relevant improvements affecting (near surface) weather forecasts that have been implemented at MeteoSwiss include a new 2m temperature diagnostics (Buzzi 2008), an improved new soil model and external parameters (Heise et al. 2006), a new horizontal grid with 6.6km mesh size with a new lowest model layer at 10m and the introduction of a sub-grid scale orography scheme (Schulz 2008, deVries 2009) to better account for surface variability within a model grid box. As may reasonably be presumed, predictive building automation applications will benefit from these model improvements as the controller will have to mitigate smaller prediction error. Therefore, the OptiControl Weather and Occupancy Database has been updated with the newest COSMO-7 predictions and associated observations for the Swiss stations. This extended version of the database will enable long-term simulations at specific sites to learn more about the sensitivity of the controller applications to weather forecast errors (chapter 4.2). In addition, the new datasets for Basel will be input for a validation study for the simulation of the demonstrator building (Sagerschnig 2010).

6.2 Data availability OCWDB 1.9

According to the needs of the envisaged simulations with BACLab (Sagerschnig et al 2010, chapter 4.2), the new datasets of meteorological measurements and COSMO-7 predictions comprise all relevant weather variables for the four Swiss stations and the years 2008 and 2009. Also, the data for the dewpoint temperature and the surface albedo that are necessary as input for the radiation conversion are added for the years 2006 and 2007 in order to provide the meteorological input for long-term building simulations that will be particularly appealing for the demonstrator building. For an overview of the available datasets in OCWDB 1.9 see
Table ***9.1*** in the appendix.

7 Literature

Buzzi M (2008) *Challenges in operational numerical weather prediction at high resolution in complex terrain*. Dissertation, Diss. ETH No. 17714, ETH Zurich, Switzerland, 185p.

Cattani D (1994) Application d'un filtre de Kalman pour adapter les températures à 2 mètres fournies par le modèle ECMWF aux stations météorologiques de la Suisse. Rapports de travail de l'Institut Suisse de Météorologie, no 175.

Erbs DG, Klein SA, Duffie JA (1982) Estimation of the diffuse radiation fraction for hourly, daily and monthly-average global radiation. *Solar Energy*, 28 (4), 293-302.

Gwerder M, Gyalistras D, Oldewurtel F, Lehmann B, Wirth K, Stauch V, Tödtli J (2010) Potential assessment of rule-based control for Integrated Room Automation. Paper presented at the 10th REHVA World Congress Clima 2010, 9-12 May 2010, Antalya, Turkey, 8pp.

Heise E, Ritter B, Schrodin R (2006) Operational implementation of a multilayer soil model. COSMO Technical report No 9.

Ineichen P (2008) Comparison and validation of three global-to-beam irradiance models against ground measurements. *Solar Energy*, 82, 501-512.

Kalman RE (1960) A New Approach to Linear Filtering and Prediction Problems, *Transactions of the ASME–Journal of Basic Engineering*, Vol 82.

Merkblatt SIA 2028 *Klimadaten für Bauphysik, Energie- und Gebäudetechnik* (2008).

Oldewurtel F, Gyalistras D, Gwerder M, Jones CN, Parisio A, Stauch V, Lehmann B, Morari M (2010) Increasing Energy Efficiency in Building Climate Control using Weather Forecasts and Model Predictive Control. Paper presented at the 10th REHVA World Congress Clima 2010, 9-12 May 2010, Antalya, Turkey, 8pp.

Perez R, Ineichen P, Maxwell E, Seals R, Zelenka A (1992) Dynamic global to direct conversion models. *ASHRAE transactions, Research Series* 1992, 354-369.

Perez R, Seals R, Ineichen P et al. (1987) A new simplified version of the Perez diffuse irradiance model for tilted surfaces, *Solar Energy*, 39 (3), 221-231.

Reindl DT, Beckman WA, Duffie JA (1990) Diffuse fraction correlations. *Solar Energy*, 45 (1), 1-7.

Sagerschnig, C., Gyalistras, D., Gwerder, M. & Seerig, A. (2010). The OptiControl demonstrator building: Description, modeling and energy savings potential of predictive control. Technical Report, Building Climate Control, Gruner AG, Basel.

Schulz JP (2008) Introducing sub-grid scale orographic effects in the COSMO model. COSMO Newsletter No 9.

Skartveit A, Olseth JA (1987) A model for the diffuse fraction of hourly global radiation. *Solar Energy*, 38 (4), 271-274.

Stauch VJ, Gwerder M, Gyalistras D, Schubiger F (2008) Statistical adaptation of mesoscale numerical weather forecasts for designing predictive control of indoor building climates. In: Proc. 8th Annual Meeting of the EMS and 7th European Conference on Applied Climatology, 29 September - 3 October 2008, Amsterdam, The Netherlands, Vol. 5, EMS2008-A-00545

Stauch VJ, Schubiger F, Steiner P (2010) Local weather forecasts and observations. In: Gyalistras, D., Gwerder, M. (Eds.): Use of weather and occupancy forecasts for optimal building climate control (OptiControl): Two years progress report. Terrestrial Systems Ecology ETH Zurich, Switzer-land and Building Technologies Division, Siemens Switzerland Ltd., Zug, Switzerland.

Steppeler J, Doms G, Schättler U, Bitzer H, Gassmann A, Damrath U, Gregoric G (2003) Meso-gamma scale forecasts using the non-hydrostatic model LM. *Meteorology and Atmospheric Physics*, 82, 75-96.

deVries A (2009) *Parametrization of Subgrid-Scale Orographic Drag in a Numerical Weather Prediction Model*, master thesis supervised by O Fuhrer and C Schär, Institute of Atmospheric and Climate Science, ETH Zurich, Switzerland.

8 Acknowledgements

The meteorological observations at the European stations have been provided by the national weather services and we are particularly grateful to:

- French Weather Service (MeteoFrance) for providing us with the observations at the measurement sites Marseille-Marignane and Clermont-Ferrand
- German Weather Service (DWD) for providing us with the observations at the measurement sites Mannheim and Hohenpeissenberg
- Austrian Weather Service (ZAMG) for providing us with the observations at the measurement site Wien Hohe Warte
- Italian Weather Service for Emilia-Romagna (ARPA-SIM) for providing us with the observations at the measurement site Modena

9 Appendix

9.1 Abbreviations for selected sites

BAS	Basel, Switzerland
GVE	Geneva, Switzerland
LUG	Lugano, Switzerland
SMA	Zurich (Fluntern), Switzerland
WHW	Vienna (Hohe Warte), Austria
MSM	Marseille (Marignane), France
CLF	Clermon-Ferrand, France
MHM	Mannheim, Germany
HPB	Hohenpeissenberg, Germany
MOD	Modena, Italy

For more information see Stauch et al. (2010)

9.2 Abbreviations for the relevant weather variables

ALB	surface albedo
RG	global radiation (W m^{-2})
RGE	global radiation vertical east (W m^{-2})
RGN	global radiation vertical north (W m^{-2})
RGS	global radiation vertical south (W m^{-2})
RGW	global radiation vertical west (W m^{-2})
TA	air temperature at 2m above ground (°C)
TD	dew point temperature at 2m above ground (°C)
dSolG	solar heat gain of a room (W m^{-2})
Tfreecool	free cooling temperature (°C)

For more information see Stauch et al. (2010)

9.3 Table of data availability for COSMO-7 predictions and observations

Table 9.1: Availability of the weather predictions and observations in OCWDB 1.8

year	site	TA	TW	TD	RG	RGE	RGS	RGW	RGN	ALB	other sia
DRY-mean	BAS	x	x	x	x	x	x	x	x	x	x
DRY-mean	GVE	x	x	x	x	x	x	x	x	x	x
DRY-mean	SMA	x	x	x	x	x	x	x	x	x	x
DRY-mean	LUG	x	x	x	x	x	x	x	x	x	x
DRY-mean	WHW	x	x	x	x	x	x	x	x	x	x
DRY-mean	CLF	x	x	x	x	x	x	x	x	x	x
DRY-mean	MSM	x	x	x	x	x	x	x	x	x	x
DRY-mean	MHM	x	x	x	x	x	x	x	x	x	x
DRY-warm	BAS	x	x	x	x	x	x	x	x	x	x
DRY-warm	GVE	x	x	x	x	x	x	x	x	x	x
DRY-warm	SMA	x	x	x	x	x	x	x	x	x	x
DRY-warm	LUG	x	x	x	x	x	x	x	x	x	x
DRY-cold	BAS	x	x	x	x	x	x	x	x	x	x
DRY-cold	GVE	x	x	x	x	x	x	x	x	x	x
DRY-cold	SMA	x	x	x	x	x	x	x	x	x	x
DRY-cold	LUG	x	x	x	x	x	x	x	x	x	x
2006	BAS	x	x	x	x	x	x	x	x	x	x
	GVE	x	x	x	x	x	x	x	x	x	x
	SMA	x	x	x	x	x	x	x	x	x	x
	LUG	x	x	x	x	x	x	x	x	x	x
	WHW	x	x	x	x	x	x	x	x	x	x
	CLF	x	x	x	x	x	x	x	x	x	x
	MSM	x	x	x	x	x	x	x	x	x	x
	HPB	x	x	x	x	x	x	x	x	x	x
	MHM	x	x	x	x	x	x	x	x	x	x
	MOD	x	x	x	x	x	x	x	x	x	x
2007	BAS	x	x	x	x	x	x	x	x	x	-
	GVE	x	x	x	x	x	x	x	x	x	-
	SMA	x	x	x	x	x	x	x	x	x	-
	LUG	x	x	x	x	x	x	x	x	x	-
	WHW	x	x	x	x	x	x	x	x	x	-
	CLF	x	x	x	x	x	x	x	x	x	-
	MSM	x	x	x	x	x	x	x	x	x	-
	HPB	-	-	-	-	-	-	-	-	-	-
	MHM	-	-	-	-	-	-	-	-	-	-
	MOD	x	x	x	x	x	x	x	x	x	-
2008	BAS	x	x	x	x	-	-	-	-	x	-
	GVE	x	x	x	x	-	-	-	-	x	-
	SMA	x	x	x	x	-	-	-	-	x	-
	LUG	x	x	x	x	-	-	-	-	x	-
2009	BAS	x	x	x	x	-	-	-	-	x	-
	GVE	x	x	x	x	-	-	-	-	x	-
	SMA	x	x	x	x	-	-	-	-	x	-
	LUG	x	x	x	x	-	-	-	-	x	-